#### **Research Article**

Zainab S. Maarij, Tahseen D. Saadoon\*, Maan S. Hasan, and Anmar Dulaimi

# Investigation of the hydraulic characteristics and homogeneity of the microstructure of the air voids in the sustainable rigid pavement

https://doi.org/10.1515/eng-2022-0564 received October 20, 2023; accepted November 15, 2023

Abstract: The present research investigates how incorporating waste concrete block aggregates (WCBA) in place of natural coarse (5-12 mm) aggregates (NCA) affect the characteristics of concrete pavement. The topography of the voids, water absorption, porosity, and hydraulic conductivity characteristics such as flexural and compressive strengths in addition to density were investigated. The consequences of replacement were looked at using four replacement percentages, 10, 30, 60, and 100% of the normal weight had been substituted with 0% functioning as the control value. Mix design of 1:1.41:2.52 (cement:fine aggregate:coarse aggregate) was used in the study with water to cement ratio of 0.43. As the replacement percentage of WCBA increased, water absorption, porosity, and hydraulic conductivity increased while density, compressive strength, and flexural strength decreased. The drop in values in comparison to control mixture were in the range of 10-30, 22-40, and 1-32% for density, compressive strength, and flexural strength, respectively. On the other hand, increase in values (16-33, 12-40, and 11-37%) have been identified for hydraulic conductivity, porosity, and water absorption, respectively. When designing rigid pavement, concrete with replacement percentages of WCBA 30% produces results that were acceptable. Porosity along with other hydraulic characteristics, such as hydraulic conductivity, are closely associated. There is an extremely significant correlation between porosity and all topological parameters. Finally, high level validation ( $R^2$  >

0.9) and predictive models of hydraulic conductivity and porosity were established.

**Keywords:** recycled, aggregate, concrete, voids, models, topology, hydraulic conductivity

# 1 Introduction

On a global scale, 25 billion tons of concrete undergo manufacturing every year. Aggregate, a vital component that significantly impacts the qualities of concrete, make up to 80% of the volume of concrete [1]. The constructing industry's explosive growth has resulted in sustainability issues as a result of over-mining and excessive utilization of natural resources like cement and aggregate [2]. Under such pressure, industries - particularly the construction industry, which has adverse environmental consequences due to its enormous consumption of natural resources and production of building wastes - are driven to seek out sustainable technology. Therefore, it is of utmost importance to use leftover construction debris to create environmentally friendly materials. Concrete may be manufactured by partially or entirely substituting recycled aggregate (RA) for natural aggregate (NA).

Due to its low compressive strength and high degree of variation, recycled aggregate concrete (RAC) is recommended for non-structural concrete or pavement applications [3–5]. The pores in the structures are enlarged and increased by the hardened mortar that is connected to the surface of the RAs, which lowers the density of the aggregate and raises its water absorption above NA [2]. Because of this, it is challenging to manage the toughened RAC's durability and adaptability. The inferior performance of RAC in comparison to natural aggregate concrete has been supported by earlier studies [3–5]. Because aggregate makes up a larger portion of concrete's components, its properties will have a significant impact on how voids and pores are arranged, which will affect how liquids are transferred into and out of concrete.

**Zainab S. Maarij:** Civil Engineering Department, University of Technology-Iraq, Baghdad, Iraq

**Maan S. Hasan:** Civil Engineering Department, University of Technology-Iraq, Baghdad, Iraq

**Anmar Dulaimi:** University of Kerbala, University of Warith Al-Anbiyaa, Kerbala, Iraq

<sup>\*</sup> Corresponding author: Tahseen D. Saadoon, Civil Engineering Department, University of Technology-Iraq, Baghdad, Iraq, e-mail: Tahseen.D.Saadoon@uotechnology.edu.iq

Specifically, in cement concrete pavement, due to high surface area and contact with base layer (unbound material), there is a significant chance to ingress aggressive materials inside pavement from upper and lower surface, in addition to the sides of the pavement. Durability is one of the basic and necessary items in continuity optimum performance of concrete. The major factor in durability is the concrete's hydraulic characteristics.

Despite several studies on RAs for concrete production being conducted [6–9], the impact of RA concrete on the hydraulic properties and microstructure of the concrete voids created by RAC is yet unclear. Therefore, in this study, the effects of replacing some or all of the NA with waste crushed concrete block aggregates were evaluated in terms of compressive strength, topography of voids, water absorption, porosity, and hydraulic conductivity. After that, predictive models for the hydraulic properties of the stiff pavement created by RAC is developed.

# 2 Theoretical considerations

Distinct topology characteristics that have an impact on other distinct qualities of a concrete mixture, like hydraulic conductivity, can be used to define the air void structure within a concrete [10,11]. Tortuosity, circularity, roundness, aspect ratio, surface area, number of voids, voids class, and pore size distribution index are characteristics related to the topology of the voids structure. Based on measurements collected by X-ray computed tomography (CT) scans, these properties can be computed using universal equations (as detailed later in the current work).

# 3 Experimental details

#### 3.1 Materials

The materials used in this experiment included sulfate-resisting Portland cement, sand and gravel (fine and coarse aggregate, respectively), tap water, and superplasticizer type F (SP). Every concrete component complies with the standards used in the current study [12–15].

Since there is a substantial volume of waste concrete block in the researchers' region and because it is simple to crush, waste concrete block was crushed and sieved to produce 5–12 mm (Figure 1) sized recycled coarse aggregate. Based on past investigations, a 5–12 mm aggregate



Figure 1: (a-d) Waste concrete block is recycled to create coarse aggregate (5-12 mm).

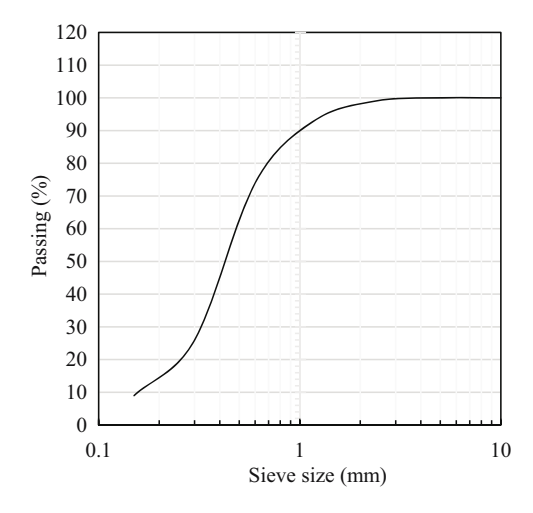


Figure 2: Gradation of fine aggregate.

size was selected [16], which, when compared to another size (12–19 mm), demonstrated increased strength.

Figures 2 and 3, respectively, show the gradations of fine (sand) and coarse (natural and waste concrete block) aggregate. Figure 4 displays the particle size and texture of both natural and recycled coarse aggregates.

The mass per unit volume of dry aggregate that has been compressed by rodding under standardized conditions is known as dry-rodded density. This volume comprises both the volume of the individual particles and the space between them. The advantage of dry-rodding is that it gives a more precise indication of the density of the aggregate than other techniques. It also makes sure that the aggregate is compacted uniformly. The specific gravities of NA and waste concrete block aggregates (WCBA), which were their dry-rodded densities, were 2.70 and 2.53, respectively. Compared to NA, WCBA had around two times higher water absorption rate.

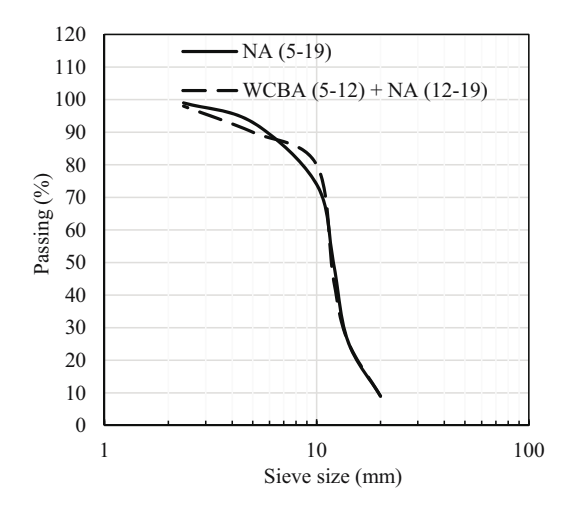


Figure 3: Gradation of coarse aggregate.

The resilience of aggregates to abrasion and impact is gauged by the Los Angeles abrasion loss value. Los Angeles abrasion values for good aggregates that are suitable for high-quality pavement materials should be lower than 30%. Loss values between 25 and 55% (or 45% in other states) are typically considered acceptable. NA and WCBA suffered Los Angeles abrasion losses of 33.2 and 48.0%, respectively.

According to earlier researchers, the RA's low-density, high-water absorption, and high Los Angeles abrasion loss were caused by the material's large porosity from the adhering cement mortar. For the aggregate test, AASHTO T19M, ASTM C127, and ASTM C131 [17–19] were used.

# 3.2 Designing a mix and preparing samples

Before mixing, the aggregates were brought to a saturated surface dry (SSD) condition. WCBA was used in place of NA



Figure 4: Samples of coarse aggregate: natural (a) and recycled (b).

with a size range of 5–12 mm at weight percentages of 0, 10, 30, 60, and 100%. The ASTM C143 standard was followed to determine the fresh concrete slump test [20]. The slump measurements varied from 100 to 110 mm. Table 1 contains a list of all mixtures' weights.

In two to three layers, the freshly prepared mixture was added to the mold. Then, a vibrating table was used to apply the compaction vibration for 15 s. All samples were demolded after 24 h and kept in a wet environment until testing.

# 3.3 Testing specifics

#### 3.3.1 Density

According to ASTM C642 [21], the density was estimated. In this test, 150 mm diameter cube specimens were employed. This test was carried out at several times: 3, 7, 28, 63, and 90 days. From the following equation, the density can be determined:

Dry density(kg/m<sup>3</sup>) = 
$$\left(\frac{w_1}{w_2 - w_3}\right) \times \rho_w$$
, (1)

where  $w_1$  is the oven dried weight of the specimen, (kg)  $w_2$  is the SSD of specimen, (kg)  $w_3$  is the submerged weight of the specimen, (kg)  $\rho_w$  is the density of water, (kg/m<sup>3</sup>).

#### 3.3.2 Water absorption

According to ASTM C642, a water absorption test was conducted [22]. 100 mm cube specimens were tested at ages of 7 and 28 days. The following equation was used to determine the water absorption:

Water absorption(%) = 
$$\frac{(B-A)}{A} \times 100$$
, (2)

where A is the oven dry weight, (g) B is the SSD weight, (g).

#### 3.3.3 Vacuumed saturated porosity test

Particularly when the replacement amount is small, the standard vacuum analysis is susceptible to the substitution of WCBA for conventional coarse aggregate. Concrete disks measuring  $60 \times 10 \pm 3$  mm were vacuumed using 100 mb for 3 h, then were vacuumed for another 2 h with saturated Ca(OH) $_2$  solution, and then left to dry for another day (Figure 5). This was done to make sure that all the pores in the concrete test specimens were completely saturated.

$$P = \frac{B - A}{B - C} \times 100\%,$$
 (3)

where P is the porosity, B is the SSD weight, A is the ovendry weight, and C is the saturated submerged weight.

#### 3.3.4 X-ray CT scans

Using a Phoenix  $v \mid tome \mid xL$  scanner, the test samples utilized for the porosity tests were scanned. A current of



Figure 5: Vacuum set up.

Table 1: Mix proportion of the concrete mixes (kg/m<sup>3</sup>)

Mix ID	Cement (kg/m³)		Aggregate (kg/r	n³)	SP, (kg/m³)	Water/cement	
		Fine	Co	arse			
			Natural	Recycled			
0% WCBA	450	635	1,135	0	2.4	0.33	
10% WCBA			1021.5	113.5		0.34	
30% WCBA			794.5	340.5		0.36	
60% WCBA			454	681.0		0.37	
100% WCBA			0	1,135		0.41	

1,300 A and an acceleration voltage of 290 kV were used to run the X-ray source. The test samples were scanned on a rotating platform with a 906.84 mm gap between them and the X-ray source. The exceptional resolution, which also applied to consecutive slides, was 96 m/pixel. The 16-bit photos were converted into 8-bit greyscale resolution and cropped into a region of interest (ROI) of 664 cm<sup>3</sup> using the programs Avizo 8.1 and ImageJ, Version 1.49 [23]. The noise in the photos was then reduced using a 3D Gaussian and Median filter with a  $1 \times 1 \times 1$  kernel size. Segmenting the materials in the ROI allowed for the preparation of reconstructions of the microstructure.

The BoneJ particle analyzer plugin (Version 1.3.11) in ImageJ software was used to ascertain the topological (microstructure) properties of voids that is defined and calculated later [24]. The analyze Skeleton and Skeletonize 2D/3D modules in ImageJ were used to measure the length of macropores [24].

#### 3.3.4 Hydraulic conductivity test

At room temperature (20 ± 2°C), samples' hydraulic conductivity was measured using the Florida Method (falling head method) [25] as shown in Figure 6.

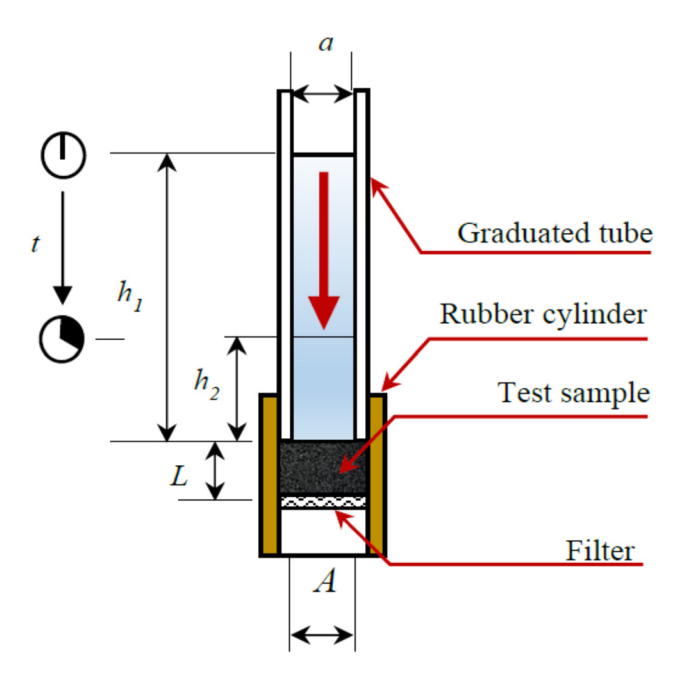


Figure 6: Scheme of hydraulic conductivity test.

Table 2: Summary of the mechanical behavior tests

Concrete test samples were cured at a temperature of 20 ± 2°C and evaluated for various curing durations. Sample and testing water were preconditioned for 4h at 20 ± 1°C before the test. The samples were then put into cylinders that were vertical and had the bottom side blocked. To completely saturate the sample, enough water was added from the top until a reference level was reached, then it was allowed to sit for 3 h. When that period was over, more water was injected to raise the reference level. After clearing the obstruction on the bottom side, the water was allowed to flow through the sample. 700 mL of water had to flow through the sample in a certain amount of time, or "t," in order to determine the hydraulic conductivity, or "Ks," according to Darcy's law [25].

$$K_{\rm S} = \frac{aL}{At} \ln \left( \frac{h_1}{h_2} \right),\tag{4}$$

where a is the inner cross-sectional area of the graduated tube (cm $^2$ ), L is the thickness of the test sample (cm), A is the test sample cross-sectional area (cm<sup>2</sup>),  $h_1$  is the initial head across the test specimen (cm), and  $h_2$  the is the final head across the test specimen (cm).

#### 3.3.5 Mechanical strength

Compressive and flexural strength tests, which are key fundamental evaluations of mechanical performance, were used to examine the concrete as shown in Table 2 and Figure 7.

# 4 Results and discussion

# 4.1 Density

Figure 8 displays the density test results for concrete. The specific gravity of recycled aggregates (WCBA) was significantly lower than that of NA, which is related to adhered mortar that was less solid and contained more voids than NA. As a result, the density of concrete decreased as the amount of RA increased. The drop was more pronounced when utilizing 100WCBA as its density (2,263), however it was still marginally lower than that of 10WCBA (2,610).

Test	Specifications followed in the test	Size of samples (mm)	Age (days)
Compressive strength	BS EN 12390 1881: part 116 [26]	Cube: 150	3, 7, 28, 63, and 90
Flexural (modulus of rupture) Strength	ASTM C78 [27]	Prismatic (100 × 100 × 400)	7 and 28



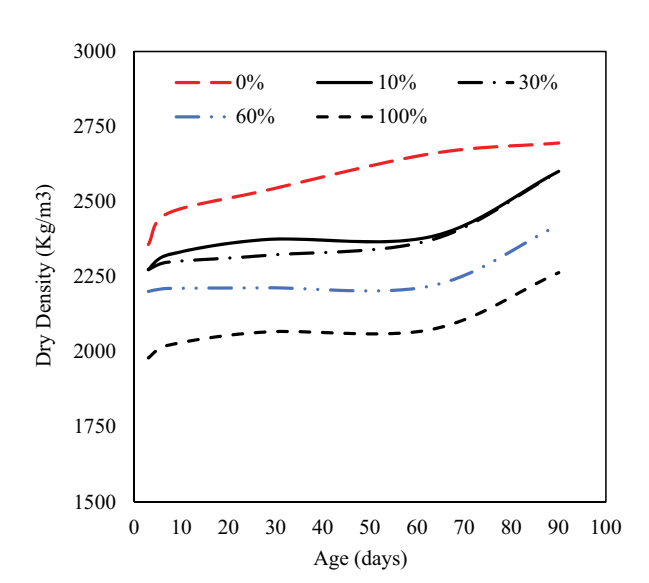


Figure 7: Samples under compressive strength test (left) and flexural strength test (right).

# 4.2 Water absorption

Considering Figure 9, the water absorption of all the WCBA-containing mixes was pretty similar at 5.33–6.67% in comparison to 4.49% of the control concrete. It should be underlined that all mixtures had the same mix proportion and particle sizes. A portion of the surface of WCBA was

formed of dry mortar, which decreased its strength, as indicated by the largest Los Angeles abrasion loss value of 48%, which was previously mentioned. While being blended, the WCBA particles underwent surface abrasion and particle crushing, which caused a sizable loss. As a result, the paste content of WCBA-concrete increased. According to that, more paste filled the gaps as the WCBA level increased,



**Figure 8:** Samples of concrete that contain various amounts of recycled coarse aggregate: Age and dry density relationship.

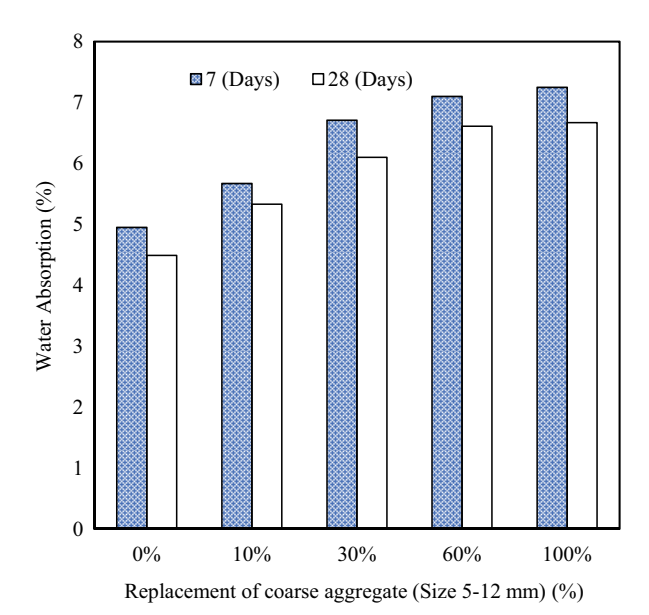


**Figure 9:** Samples of concrete that contain various amounts of recycled coarse aggregate: Age and water absorption relationship.

giving rise to WCBA-concrete with water absorption roughly equivalent to that of the control concrete. This demonstrated that the substitution of WCBA for NA had no impact on the concrete void.

A correlation between density and water absorption of WCBA-containing concretes could be discovered using the variety of WCBA-containing concrete data, as illustrated in Figure 10. The relationship is best described by Equation (1), which has an  $R^2$  value of 0.9. The preceding results that were reported are consistent with this equation [28-30].

$$W_{\rm A} = [-12.23 \times \ln D_{\rm D}] + 100.59,$$
 (5)

where  $W_A$  is the water absorption (%); and  $D_D$  is the dry density (kg/m<sup>3</sup>).

# 4.3 Porosity

Concrete porosity is the ratio of the volume of the pores to the volume of the entire concrete. Because water must evaporate after curing, leaving pores behind, concrete is a porous material. Because pores cannot support a load, a concrete's strength decreases with the increase in the porosity.

Data on the samples' porosity that were used in the current investigations are shown in Figure 11. In this scientific article, similar findings from earlier studies were validated. When additional WCBA is used in the production of concrete, it is confirmed that the porosity values increase. Considering that the porosity of concrete typically ranged from 6 to 10%, porosity levels between 10 and 60% of WCBA are regarded as appropriate.

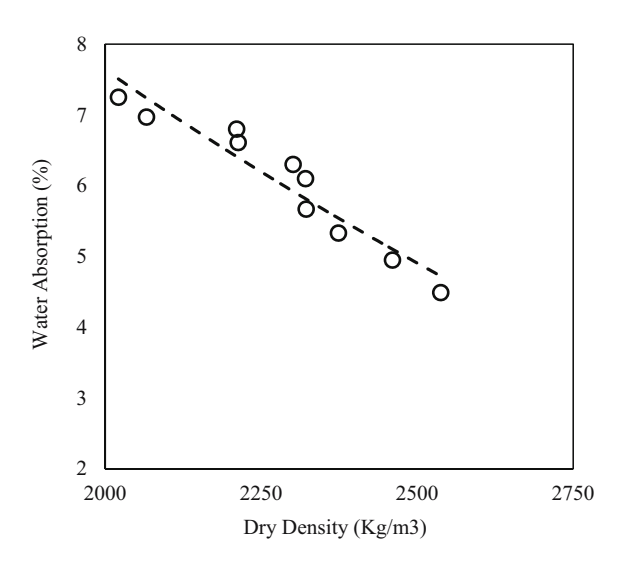


Figure 10: Absorption of water and density.

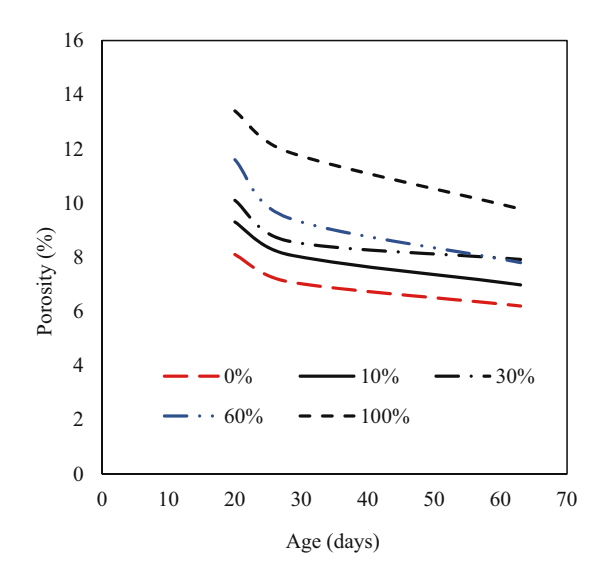


Figure 11: Samples of concrete that contain various amounts of recycled coarse aggregate: Age and porosity relationship.

# 4.4 Hydraulic conductivity

Hydraulic conductivity, also known as permeability, is a measurement of how easily fluid and gas may pass through cracks and open areas. In determining the service life of concrete structures, a significant indicator is the hydraulic conductivity of the concrete. Since permeability typically exists independent of porosity, the same effect of WCBA will be felt by both, as shown in Figures 11 and 12. Agerelated changes in porosity and mechanical strength are

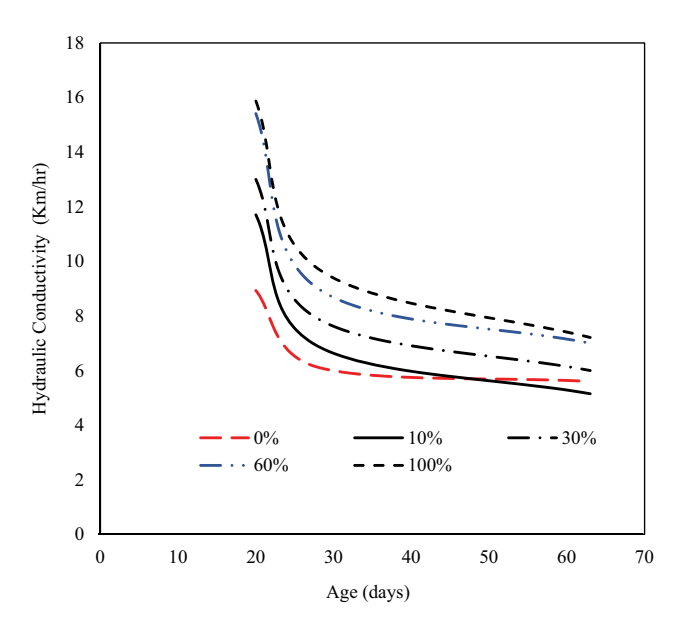


Figure 12: Samples of concrete that contain various amounts of recycled coarse aggregate: Age and hydraulic conductivity relationship.

both caused by the cement's continued hydration, which causes additional holes and voids to close and become more tightly sealed.

10% of WCBA is found in the samples, which are close replicas of the control samples. Additionally, the permeability

of samples containing 30% WCBA may in certain cases be acceptable in the field. Samples with 60 or 100% WCBA can be used as the foundation layer of pavement in areas with low water table levels, but the surface layer's concrete should be solid (low permeability).

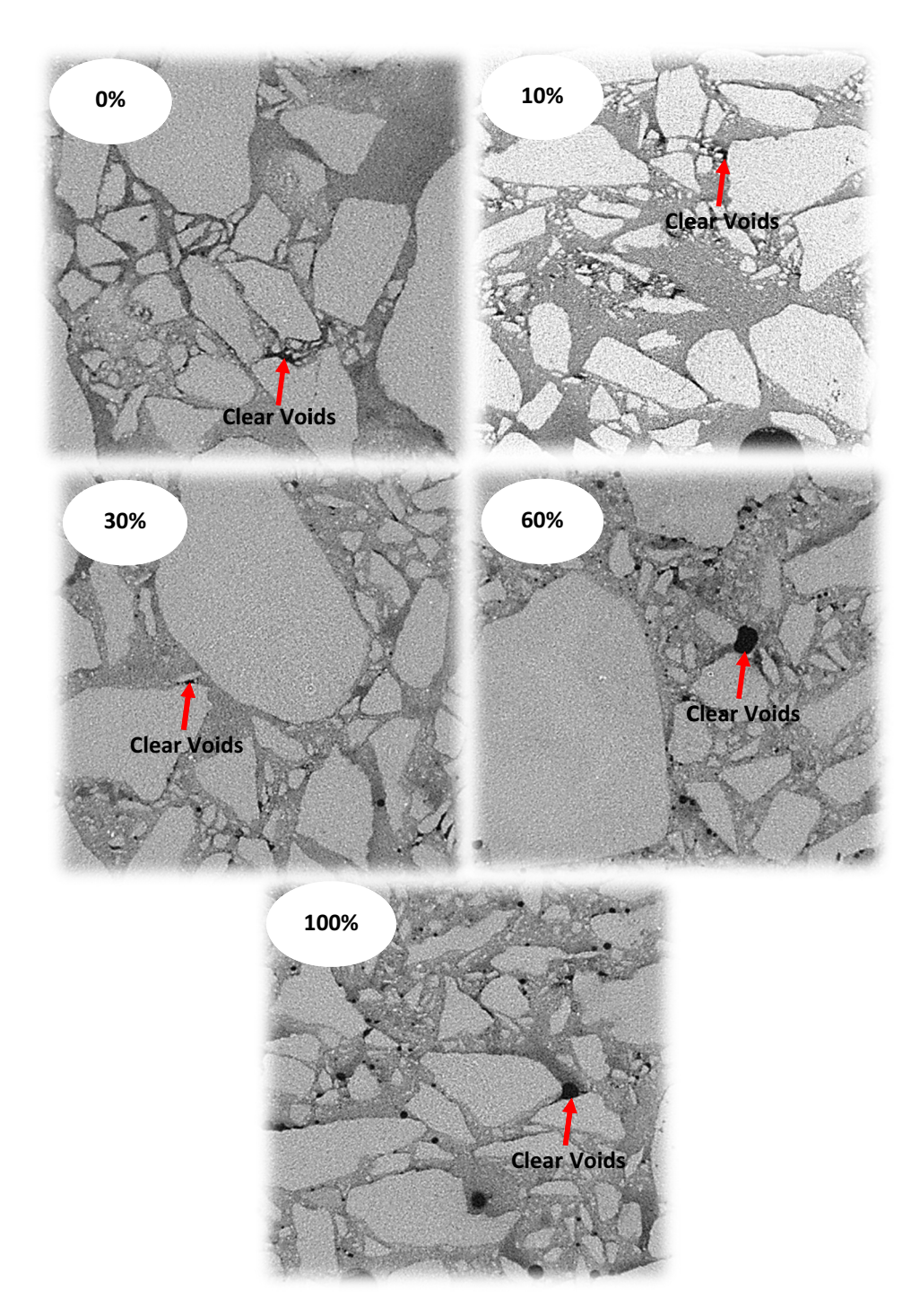


Figure 13: Some 2D slides obtained from CT scan test of the concrete samples that contain different amounts of recycled coarse aggregate.

Table 3: Parameters of the air void topology [10,31–35]

Parameter	Formula	No.
Air voids content	$A_{\rm V} = \frac{\text{Total air voids}}{\text{Total image area}} *100$	6
Circularity	$C_{i} = \frac{4 \times \pi \times \text{area of void}}{(\text{perimeter of void})^{2}}$	7
Roundness	$R = \frac{4 \times \text{area of void}}{\pi \times (\text{major axis of void})^2}$	8
Aspect ratio	$AR = \frac{Longer\ dimension}{Shorter\ dimension}$	9
Tortuosity	$T = \frac{\text{Length of pore}}{\text{Shortest distance between bore ends}}$	10
Pore size distribution index	$n = \left(\frac{k_{\rm S}}{0.003}\right)^{0.154}$	11

#### 4.5 Microstructure of air voids

Concrete's mechanical performance and durability are significantly impacted by the amount of air void in the material. The typical air void content ranges from 4 to 10%. The air void of recycled mixtures is noticeably higher than that of reference concrete.

Figure 13 provides an example of data obtained from 2D CT scan slides of concrete samples with various percentages of recycled coarse aggregate.

Tortuosity, circularity, roundness, aspect ratio, surface area, number of voids, voids content, pore size distribution index, and vertical profile are characteristics related to the

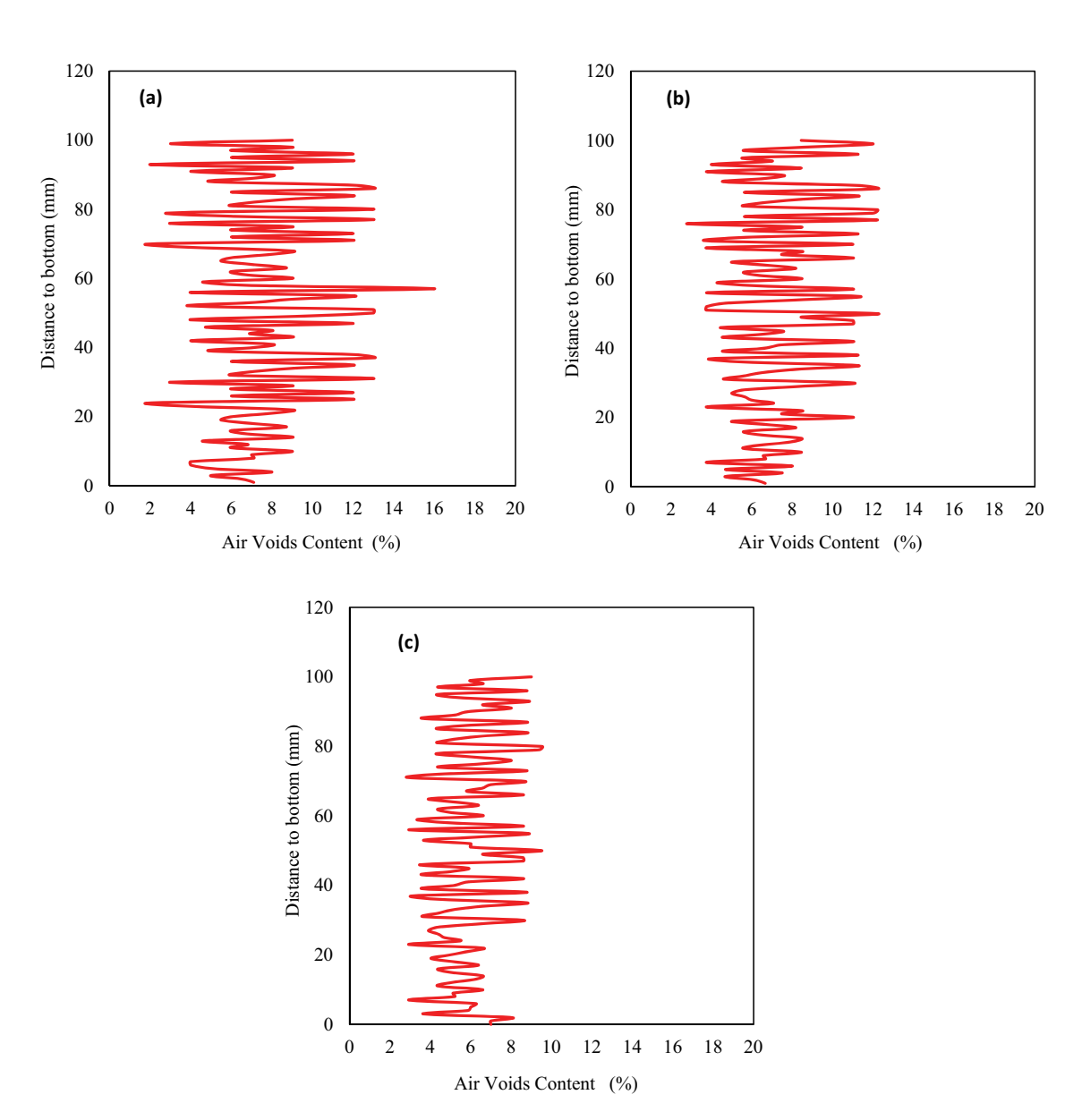
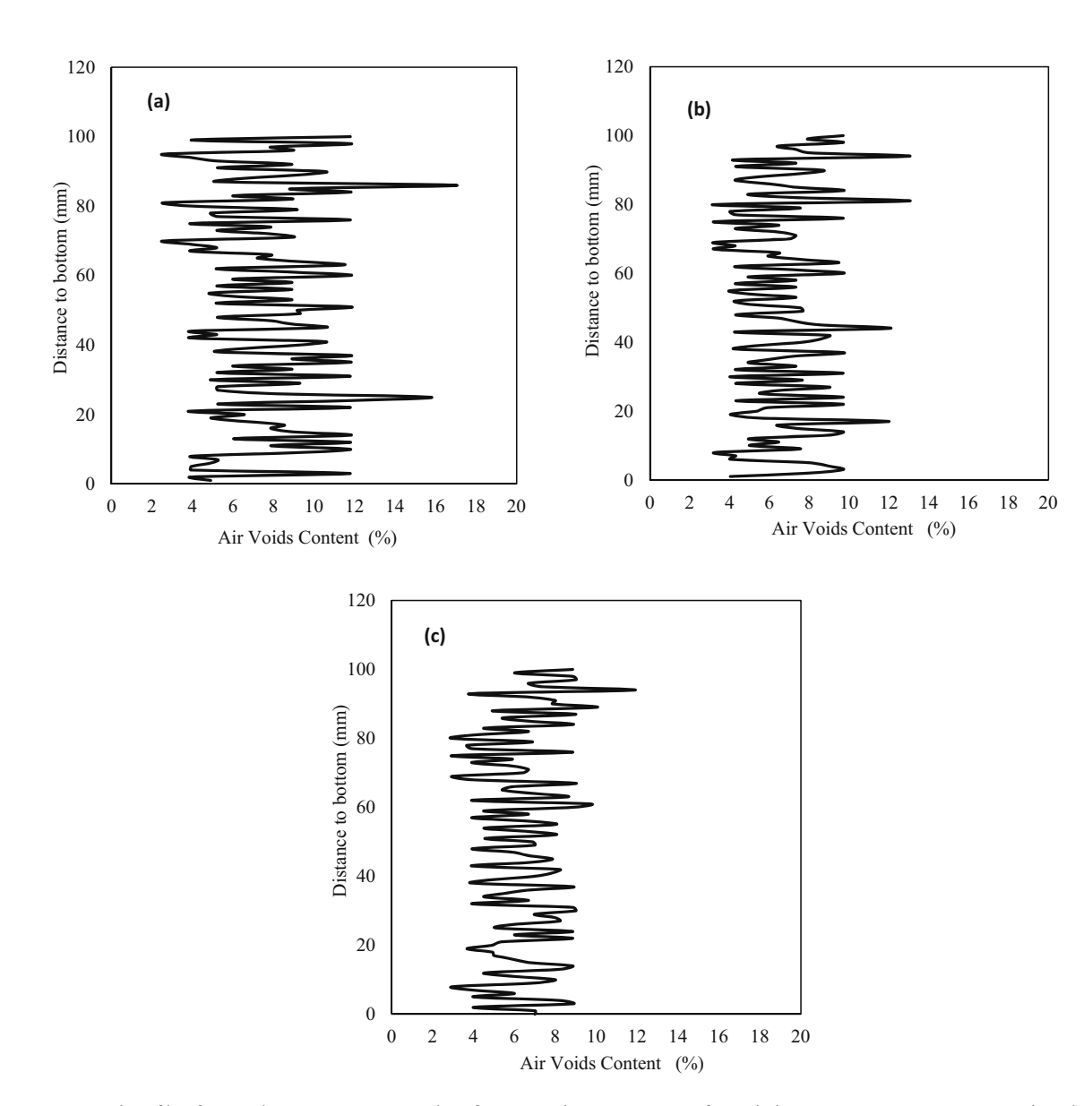


Figure 14: Vertical profile of air voids content: (a-c) Samples of control concrete at 20, 82, and 63 days, respectively.



**Figure 15:** Vertical profile of air voids content: (a–c) Samples of concrete that contain 10% of recycled coarse aggregate at 20, 82, and 63 days, respectively.

Table 4: Mean value of vertical profile of air voids content

Samples of concrete that contain various amounts of recycled coarse aggregate 0% 10% 30% 60% 100% 20 7.50% 7.58 12.80 Age 9.90 10.50 (days) 28 6.70 7.30 8.50 9.00 10.10 5.90 6.40 7.70 63 7.20 8.10

 Table 5: Standard deviation of vertical profile of air voids content

		Samples of concrete that contain various amounts of recycled coarse aggregate							
		0%	10%	30%	60%	100%			
Age	20	3.03	3.09	3.22	3.38	3.38			
(days)	28	2.57	2.29	2.16	2.26	2.96			
	63	1.82	1.94	1.92	1.91	2.33			

topology of voids structure. Using data from X-ray CT scans, these features can be estimated as given in Table 3.

Figures 14–18 and Tables 4 and 5 show the vertical profile, average, and standard deviation of air voids, respectively.

In general, the air void profiles are uniformly distributed throughout all samples. Because of this, it is possible to conclude that the qualities (such as mechanical properties, volumeweight properties, hydraulic properties, and microstructure

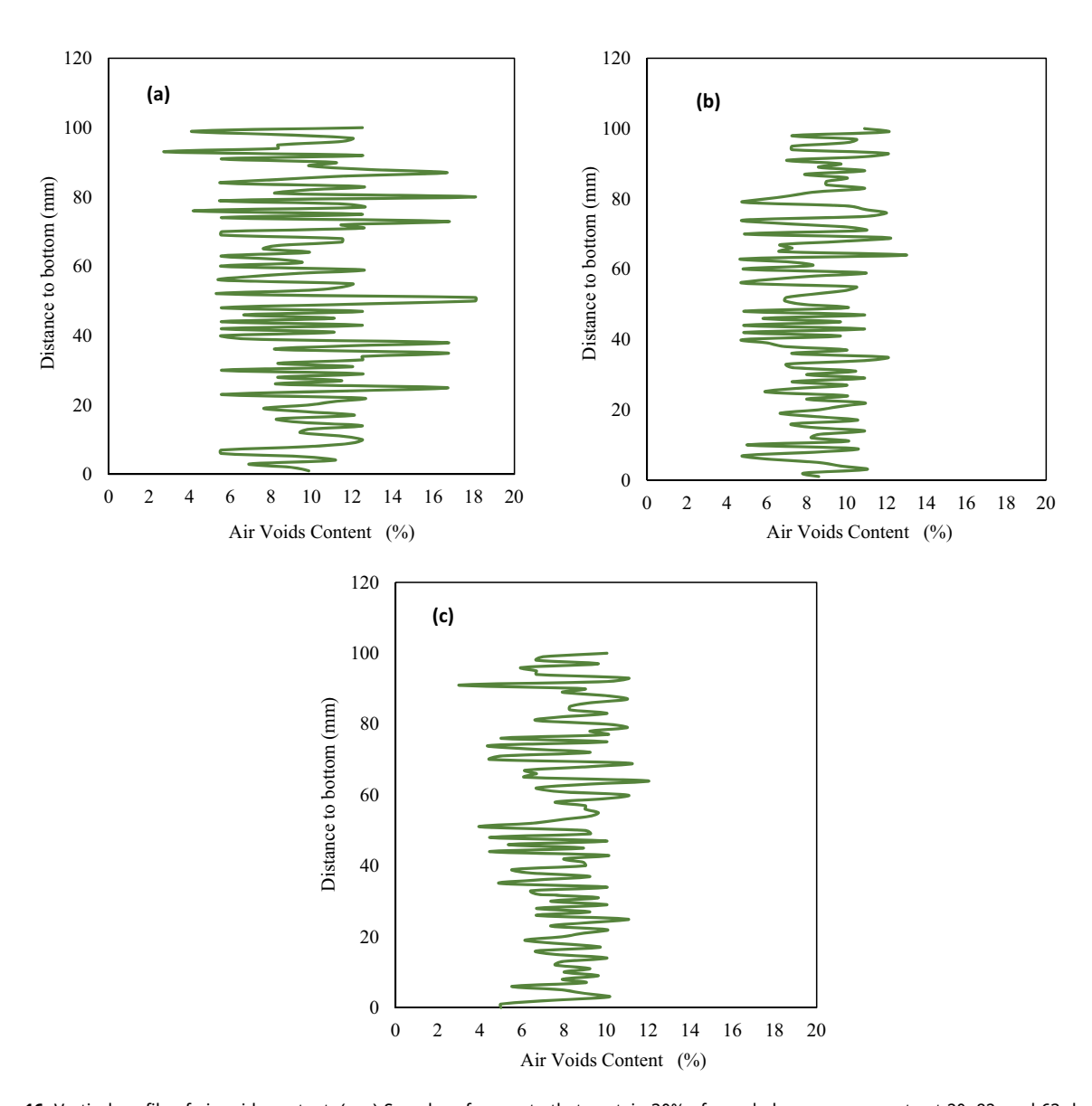


**Figure 16:** Vertical profile of air voids content: (a–c) Samples of concrete that contain 30% of recycled coarse aggregate at 20, 82, and 63 days, respectively.

characteristics) of the samples, when tested in a particular area, are indicative of the entire substance.

As can be observed, the content of voids increases as recycled WCBA are used in greater quantities. Because they are dependent on a combined component (the skeleton of pores and voids), the results of air voids content (Figures 13–17) are extremely compatible with the general conclusion of porosity (Figure 11). The majority of micropores in microstructures, particularly those that are challenging to measure in porosity tests, may be passed through and measured using CT scans. As a result, the voids content as determined by the CT-scan test was higher than the porosity test. In light of this, Figure 19 shows the proportion of small-scale voids in macrostructures.

The degree to which the routes created by the voids are twisted, winded, or turned is referred to as the tortuosity of voids in concrete. The length of the flow path is measured in relation to the length of a straight line connecting the two sites. Concrete's tortuosity can be estimated using a variety of techniques, including CT imaging. It is crucial to explore the tortuosity in the current work in light of the impact of permeability on the longevity of rigid pavement since it is a significant property that affects the permeability of concrete.

In other words, by increasing the density, the circularity increases because there is more surface tension at the voids—mortar interface in a fresh mortar. The circularity of the voids and density closely correspond with one

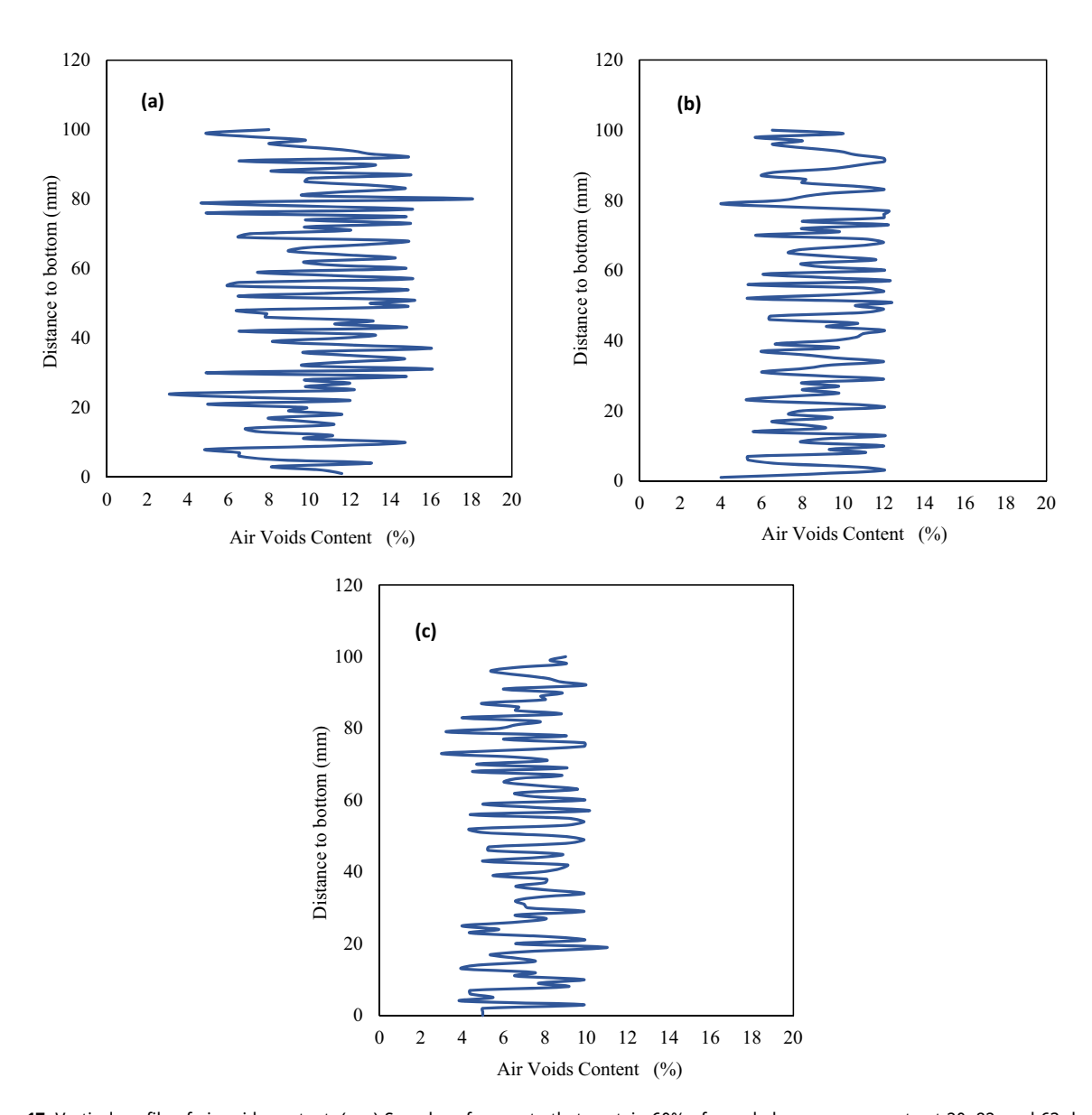


Figure 17: Vertical profile of air voids content: (a–c) Samples of concrete that contain 60% of recycled coarse aggregate at 20, 82, and 63 days, respectively.

another. Additionally, the flexural strength of the concrete was significantly influenced by the circularity of the voids, but the compressive strength was mostly influenced by the quantity of porosity.

When the air voids' circularity, roundness, and aspect ratio are all close to 1, the voids have a sphere-like structure; however, if the aspect ratio is larger and the circularity and roundness values are close to 0, the voids take on an elongated shape, as seen in Figure 20 [35].

The results of the topology of voids structure obtained from samples of the current work are shown in Table 6. With the exception of the roundness and aspect ratio parameters, all topology test variables were positively correlated with WCBA replacement quantity. Higher tortuosity,

circularity, roundness, surface area, and pore size distribution index classes will result in higher porosity and/or hydraulic conductivity, as indicated in previous research [31].

# 4.6 Mechanical performance

Figures 21 and 22 show the results of tests on the compressive and flexural strengths of concretes at various ages. The strength of concrete is among its most important qualities. Because crushed concrete block aggregate (WCBA) is used, concrete should be suitably robust.

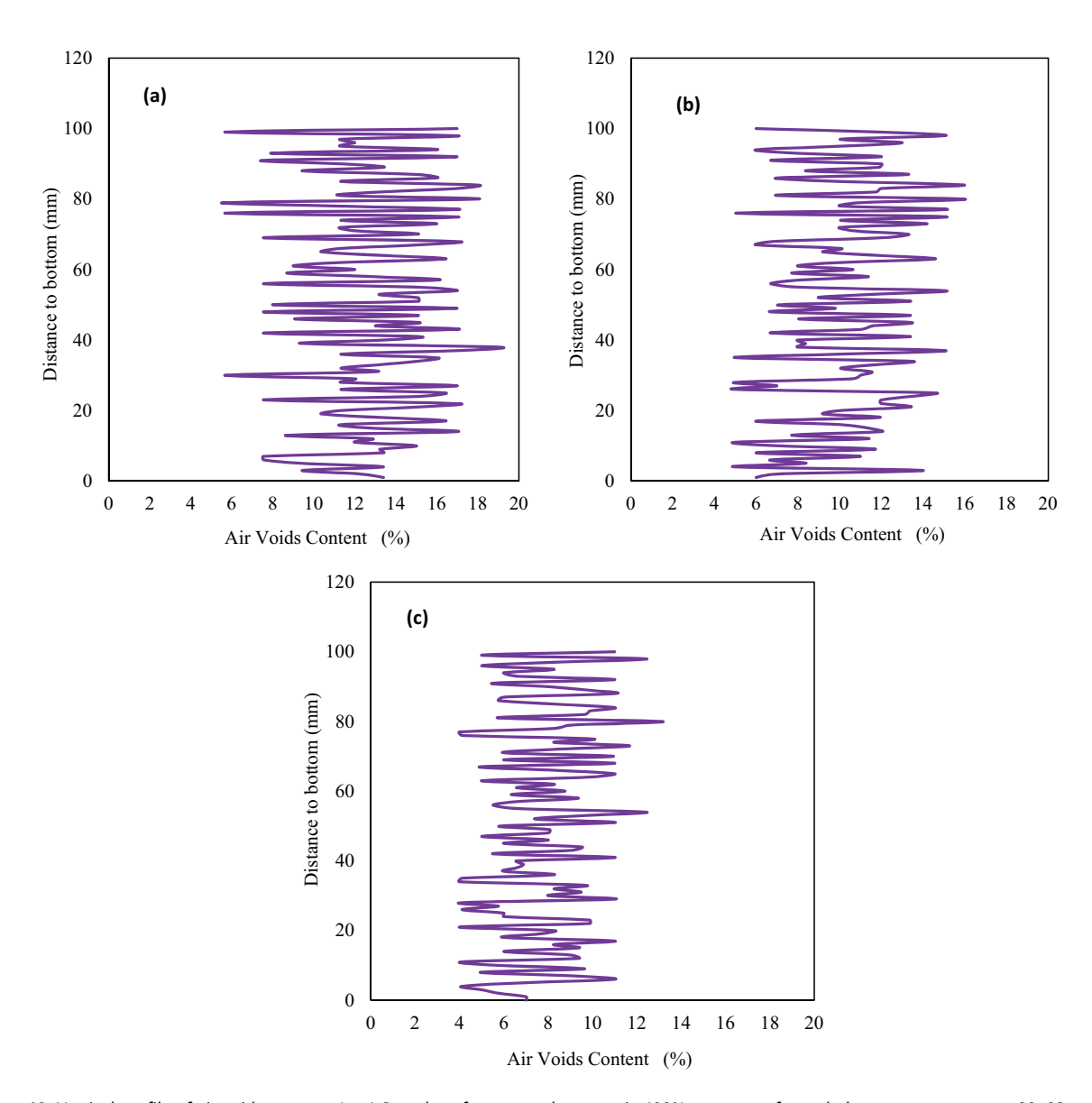


**Figure 18:** Vertical profile of air voids content: (a–c) Samples of concrete that contain 100% amounts of recycled coarse aggregate at 20, 82, and 63 days, respectively.

The strength of the concrete was decreased as a result of the WCBA microstructure. This was anticipated because the strength of concrete is usually decreased when broken concrete block aggregate is used [36–38].

Concrete with no WCBA had a suitable compressive strength at 28 days (38.9 MPa), whereas concrete with 10–100% WCBA had compressive strengths of 35.3 and 24.0 MPa, respectively. This shows that the 100% WCBA lowered the compressive strength of the control concrete to 38.3%.

As mentioned in Section 1, cement mortar is applied to RA. Because the interface between cement pastes and aggregate is weaker than the strength of aggregate, pervious concrete often cracks at the interface or the binder layer between the aggregate [39–41]. However, it is clear

that the compressive strength is decreased at high levels of recycled material replacement, therefore this should be taken into consideration.

According to test results shown in Figures 21 and 22, RAs had an impact on compressive strength, though not as much as they had on flexural strength. These qualities have a tendency to significantly deteriorate due to the high replacement levels. For instance, the flexural strengths of the control and 100% WCBA concrete were 4.6 and 4.71 MPa. The ratios of flexural to compressive strength were 12.4–14.1%, with an average of 13.25%. These ratios were just a little more than the 12.7% ratio of the control concrete.

WCBA can consequently be used in concrete, but only as a partial and not a full replacement for NA.

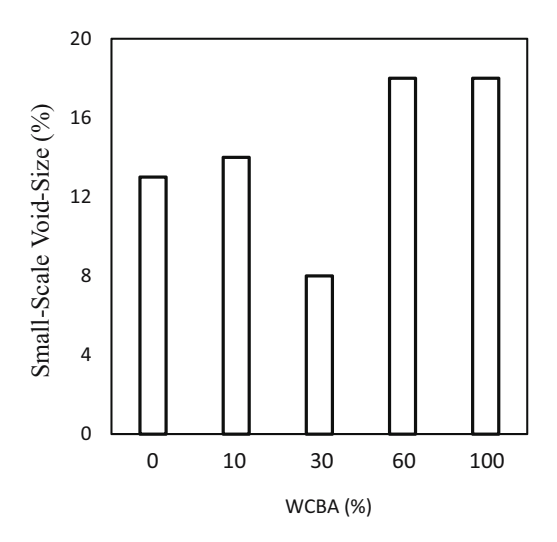


**Figure 19:** Samples of concrete that contain various amounts of recycled coarse aggregate: Small-scale void-size and WCBA.

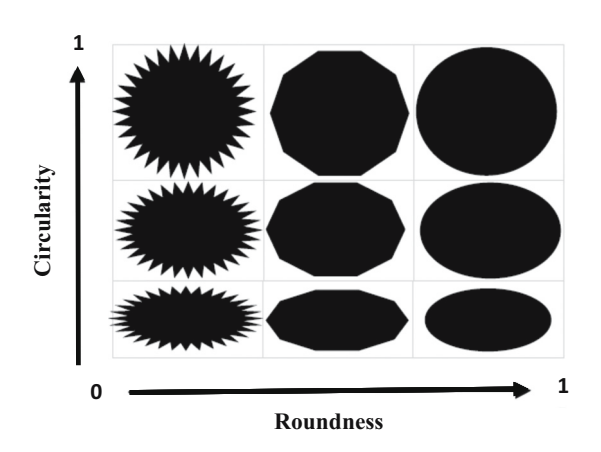


**Figure 20:** Visual description of properties related to pore topology: roundness, circularity, and tortuosity.

**Table 6:** Mean value of the topology parameters of voids of the samples of concrete that contain various amounts of recycled coarse aggregate at age of 28 days

	0%	10%	30%	60%	100%
T (-)	1.00	1.20	1.26	2.23	2.78
Ci (-)	0.42	0.35	0.28	0.26	0.23
R (-)	0.11	0.14	0.14	0.18	0.23
AR (-)	2.00	1.89	1.62	1.58	1.55
$A \text{ (mm}^2\text{)}$	1.80	1.98	2.10	2.16	2.27
N (-)	240	267	329	360	423
n (-)	1.12	1.28	1.55	1.76	2.17

Tortuosity (7), Circularity (Ci), Roundness (R), Aspect ratio (AR), Surface area (A), Number of voids (N), Pore size distribution index classes (n).

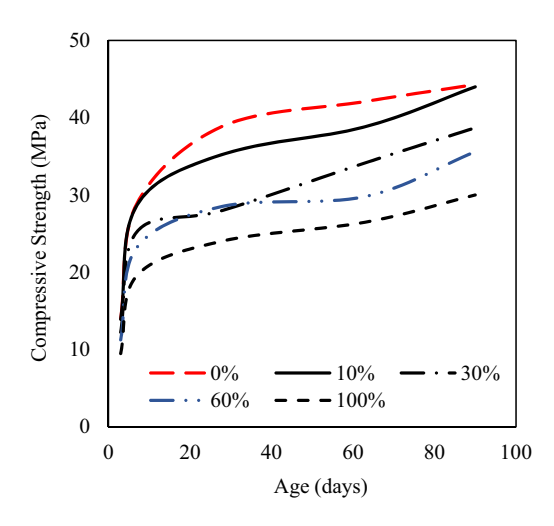


**Figure 21:** Samples of concrete that contain various amounts of recycled coarse aggregate: Age and compressive strength relationship.

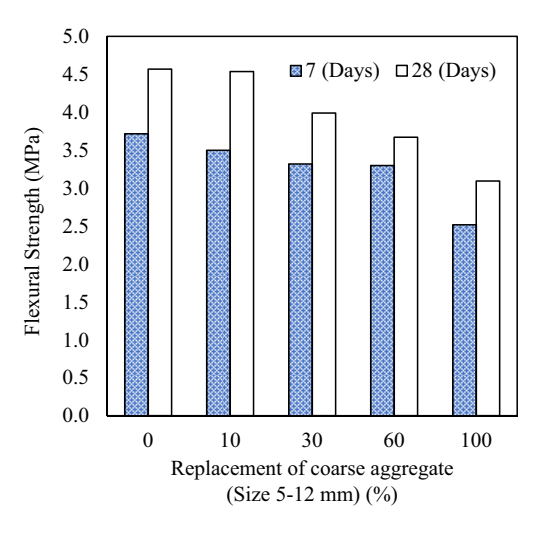


**Figure 22:** Samples of concrete that contain various amounts of recycled coarse aggregate: Age and flexural strength relationship.

# 4.7 Correlations between properties obtained for tested samples

Pearson's correlation coefficients ( $R^2$ ) were used to analyze and describe the correlation between the various parameters under investigation. The range of this correlation coefficient is 0–1. A very low correlation exists between 0 and 0.4, a moderate correlation exists between 0.4 and 0.7, and a high or very high correlation exists between 0.7 and 1 [42].

Table 7 displays the findings of a statistical analysis using Pearson's correlation coefficients to examine the correlations between each pair of attributes.

Porosity of porous materials is closely connected with the majority of other hydraulic parameters, including hydraulic conductivity, according to earlier studies in the field [10,31].

**Table 7:** Pearson's statistical analysis (Pearson's correlation factor;  $R^2$ )

	CS (MPa)	FS (MPa)	Φ (%)	HC (km/h)	AVC (%)	T (-)	Ci (-)	R (-)	AR (-)	A (mm <sup>2</sup> )	N (-)	n (-)
CS (MPa)	1											
FS (MPa)	0.94	1.00										
Φ (%)	-0.89	-0.96	1.00									
HC (km/h)	-0.95	-0.97	0.94	1.00								
AVC (%)	-0.91	-0.98	0.89	0.93	1.00							
T (-)	-0.82	-0.95	0.95	0.95	0.89	1.00						
Ci (-)	0.98	0.91	-0.88	-0.96	-0.86	-0.83	1.00					
R (-)	-0.86	-0.95	0.99	0.95	0.87	0.98	-0.87	1.00				
AR (-)	0.98	0.90	-0.81	-0.94	-0.89	-0.79	0.98	-0.80	1.00			
A (mm <sup>2</sup> )	-0.98	-0.93	0.92	0.97	0.87	0.87	-0.99	0.91	-0.96	1.00		
N (-)	-0.97	-0.99	0.96	0.99	0.96	0.93	-0.95	0.95	-0.93	0.97	1.00	
n (-)	-0.94	-0.99	0.98	0.98	0.95	0.95	-0.93	0.97	-0.90	0.96	1.00	1.00

Compressive strength (CS), Flexural strength (FS) [12], Porosity ( $\phi$ ), Hydraulic conductivity (HC), Air voids content (AVC), Tortuosity (T), Circularity (Ci), Roundness (R), Aspect ratio (AR), Surface area (A), Number of voids (A), Pore size distribution index classes (A).

Additionally, it is quick and simple to determine. As seen in Table 7, there is a strong positive association between this characteristic (the porosity) and the hydraulic conductivity ( $R^2 = 0.94$ ). Increases in porosity can therefore be interpreted as an increase in linked pores/voids. The roundness and aspect ratio of air voids have the highest and lowest correlations with porosity, respectively ( $R^2 = 0.99$  and 0.81), among all topological constants, which have high to very high correlations with porosity.

Additionally, it has been discovered that the porosity has a positive association with all other parameters but that the circularity and aspect ratio have a negative correlation with this parameter. This phenomenon is connected to the increased porosity that occurs when the aspect ratio or circularity is decreased. Because of this, circularity or aspect ratio needs to be lowered when the purpose is to produce porous or permeable concrete pavement, and *vice versa*.

Concrete's fundamental characteristic is its ability to withstand compression. There are slabs present in the concrete pavement that are supported by the soil's foundation. Even though a high-quality system is used in construction, there is a good probability that the soil could collapse, which will cause the pavement to deflect downward. Therefore, when designing stiff pavement, flexural strength is taken into account as a necessary mechanical attribute.

Circularity and pore size distribution index classes in Table 7 had the most positive and negative effects on the flexural parameter (strength), respectively. This means that in order to increase flexural strength, voids' aspect ratio and/or circularity must be increased, while other topological qualities must be decreased.

In Table 7,  $R^2$ , the correlation between the topological parameters ranged from 0.81 to 0.99. There was some

positive association and some negative correlation. This indicates that they are not linked in the same way, making it challenging to obtain all necessary features simultaneously. That means it is important to concentrate on topological factors that have a greater impact on the desirable characteristics of stiff pavement, such as flexural strength and permeability.

#### 4.8 Predictive models

According to the high area of the upper and lower surfaces of the concrete pavement that will be in contact with the weather and soil, there is a significant chance that

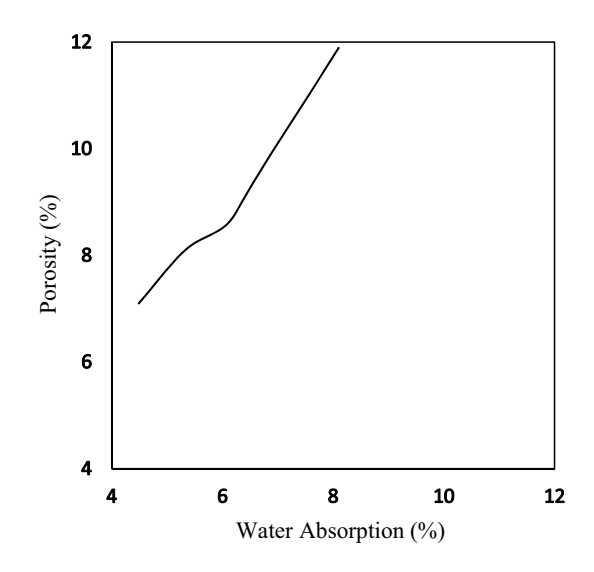


Figure 23: Correlation between water absorption and porosity.

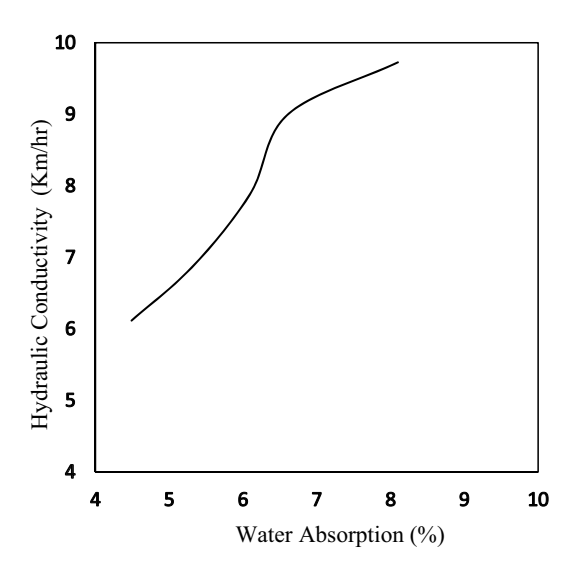
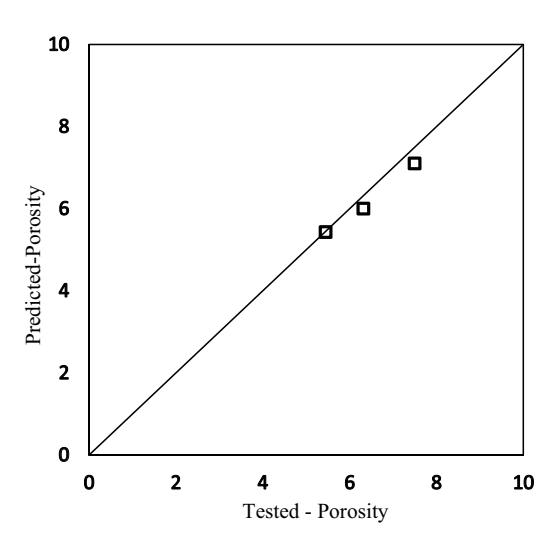


Figure 24: Correlation between water absorption and hydraulic conductivity.

aggressive materials (water table or rain) will infiltrate the concrete, which will lead to decreased performance, especially in reinforcement pavement that is caused by steel bar corrosion. Therefore, it is crucial to gauge the pavement's permeability and porosity. Predictive models are one of the feasible, time-, effort-, and money-consuming approaches for measuring attributes.

It is possible to obtain statistically approved models based on the data from the current inquiry and as shown in Figures 9, 11 and 12. The test for measuring water absorption is simple and quick, and it is connected to the same variables that affect hydraulic characteristics (such as porosity and permeability). This increases the likelihood



**Figure 25:** Comparison between predicted and tested porosity by Equation (6).

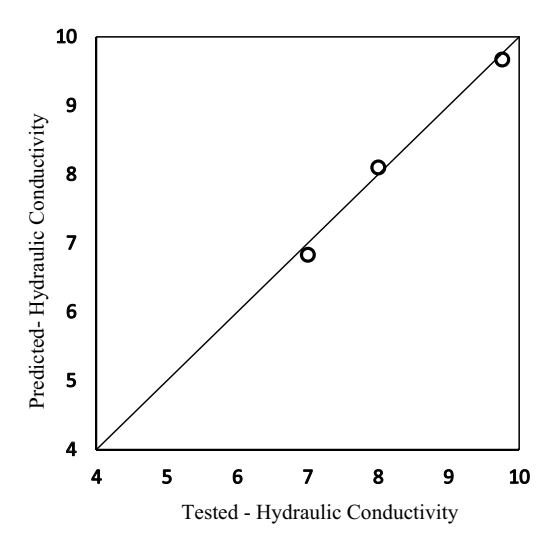


**Figure 26:** Comparison between predicted and tested hydraulic conductivity by Equation (7).

that other hydraulic features may be predicted using the data on water absorption as a known value.

Data on water absorption are correlated with porosity and permeability, respectively, in Figures 23 and 24. The power of correlation between the linked parameters is translated by the trust factor ( $R^2 = 0.95-0.97$ ), respectively. High values of this factor confirm and strengthen the conclusion that the models (Equations (6) and (7)) obtained from the earlier Figures 23 and 24 are trustworthy functions.

Porosity = 
$$1.93 \times (Water absortion)^{0.85}$$
, (6)

Hydrulic conductivity = 
$$1.74 \times (Water absortion)^{0.83}$$
. (7)

The validity of Equations (6) and (7) was discovered using new samples that contain 15, 55, and 95% WCBA. This sample can be seen as independent data because it was not utilized in the initial calibration of the model's creation. Figures 25 and 26 show the obtained validation. This makes Equations (6) and (7) more appropriate for use in other research projects, as shown by eye inspection and the correlation factor ( $R^2 = 0.98$ ).

# 5 Conclusion

Following is a summary of the study's main conclusions:

- 1. Compared to concrete made with NA, the density and mechanical strength of concrete including waste RA are lower.
- 2. The hydraulic characteristics increased when waste concrete block aggregate was used in place of NA.
- 3. When designing rigid pavement, concrete with replacement percentages of WCBA-30% produces results that are acceptable.

- 4. The key variable affecting the hydraulic characteristics is the topology of the voids.
- 5. Porosity and topological constants exhibit strong to extremely strong correlations.
- 6. Predictive models for porosity and hydraulic conductivity were obtained with a high level of validation and a high trust factor ( $R^2 > 0.9$ ).
- 7. As an outcome, it is advised to research how aggregate gradations affect void topology.

Acknowledgements: For their general assistance in the preparation, production, and testing of the specimens, the authors would like to thank the Concrete Laboratory personnel in the Department of Civil Engineering at the University of Technology-Iraq and the staff at nmRC, Concrete laboratory/ University of Nottingham/UK for their support.

**Funding information:** Authors state no funding involved.

Author contributions: All authors have accepted responsibility for the entire content of this manuscript and consented to its submission to the journal, reviewed all the results, and approved the final version of the manuscript. ZSM: data collection, experimental lab, data analysis, interpretation, and writing - original draft. TDS: conception or design, methodology, writing - review and editing, supervision, and resources. MSH: methodology, writing – review and editing, supervision, resources, and visualization. AD: writing – review and editing, supervision, and resources.

**Conflict of interest:** Authors state no conflict of interest.

Data availability statement: Most datasets generated and analyzed in this study are comprised in this submitted manuscript. The other datasets are available on reasonable request from the corresponding author with the attached information.

# References

- Fan JS. Foreign concrete block production equipment and development trend. Vol. 6, Baoding City: Hebei Province Building Materials Bureau; 1996. p. 41-2.
- Mo KH, Alengaram UJ, Jumaat MZ, Yap SP, Lee SC. Green concrete [2] partially comprised of farming waste residues: a review. J Clean Prod. 2016;117:122-38.
- Silva RV, Brito Jd, Dhir RK. Properties and composition of recycled aggregates from construction and demolition waste suitable for concrete production. Constr Build Mater. 2014:65:201-17. doi: 10. 1016/j.conbuildmat.2014.04.117.

- Antonio EB, Valdir S, Denise CC, José LD. Mechanical properties modeling of recycled aggregate concrete. Constr Build Mater. 2010;24(4):421-30. doi: 10.1016/j.conbuildmat.2009.10.011.
- Etxeberria M, Vázquez E, Marí A, Barra M. Influence of amount of [5] recycled coarse aggregates and production process on properties of recycled aggregate concrete. Cem Concr Res. 2007;37(5):735-42. doi: 10.1016/j.cemconres.2007.02.002.
- [6] Abed M, Nemes R, Tayeh BA. Properties of self-compacting highstrength concrete containing multiple use of recycled aggregate. J King Saud Univ - Eng Sci. 2020;32(2):108-14. doi: 10.1016/j.jksues.
- Miren E. The suitability of concrete using recycled aggregates (RAs) for high-performance concrete. In: Advances in construction and demolition waste recycling. Woodhead Publishing; 2020:1076-9. p. 253-84.
- Gao C, Huang L, Yan L, Jin R, Chen H. Mechanical properties of [8] recycled aggregate concrete modified by nano-particles. Constr Build Mater. 2020;241:118030. doi: 10.1016/j.conbuildmat.2020. 118030.
- Mohammed Ali AAZ, Ahmed RS, Waleed T. Evaluation of high-[9] strength concrete made with recycled aggregate under effect of well water. Case Stud Constr Mater. 2020;12:e00338. doi: 10.1016/j. cscm.2020.e00338.
- Aboufoul M, Garcia A. Factors affecting hydraulic conductivity of [10] asphalt mixture. Mater Struct. 2017;50:1-16.
- Horiba, http://www.horiba.com/fileadmin/uploads/Scientific/ Documents/PSA/Webinar\_Slides/AP027.pdf. Accessed date: 25 August 2018.
- [12] Iraqi Specifications No. (5), 1984.
- [13] Iraqi Specifications No. (45), 1984.
- [14] Iraqi Specifications No. (1431), 1989.
- [15] Iraqi Specifications No. (1703), 1992.
- Yazi M, Tung-Chai L, Kim H. Recycling of wastes for value-added applications in concrete blocks: An overview. Resour Conserv Recycl. 2018;138:298-312.
- [17] AASHTO-T19/T19M. Standard method of test for bulk density ("Unit Weight") and voids in aggregate, 2021.
- [18] ASTM C127-15. Standard test method for relative density (Specific Gravity) and absorption of coarse aggregate, 2021.
- ASTM C131/C131M-20. Standard test method for resistance to degradation of small-size coarse aggregate by abrasion and impact in the los angeles machine, 2021.
- [20] ASTM C143/C143M-20. Standard test method for slump of hydraulic-cement concrete, 2021.
- [21] ASTM C642-21. Standard test method for density, absorption, and voids in hardened concrete, 2021.
- [22] ASTM C642-21. Standard test method for density, absorption, and voids in hardened concrete, 2021.
- Abràmoff MD, Magalhães PJ, Ram SJ. Image processing with ImageJ. Biophotonics Int. 2004;11(7):36-42.
- Doube M, Kłosowski MM, Arganda-Carreras I, Cordelières FP, Dougherty RP, Jackson JS, et al. BoneJ: Free and extensible bone image analysis in ImageJ. Bone. 2010;47(6):1076-9.
- [25] Florida D. Florida method of test for measurement of water permeability of compacted asphalt paving mixtures, FM5-565. Tallahassee: Department of Transportation; 2004.
- [26] BS EN 12390 1881: part 116; Testing of hardened concrete, 2019.
- [27] ASTM C78/C78M-18; Standard test method for flexural strength of concrete (Using simple beam with third-point loading), 2022.

18

- [28] Nagataki S, Iida K, Saeki T, Hisada M. Properties of recycled aggregate and recycled aggregate concrete. International Workshop on Recycled Concrete, 2000.
- [29] Chakradhara RM. Properties of recycled aggregate and recycled aggregate concrete: effect of parent concrete. Asian J Civ Eng. 2018;19:103–10.
- [30] Elhakam AA, Mohamed AE, Awad E. Influence of self healing, mixing method and adding silica fume on mechanical properties of recycled aggregates concrete. Constr Build Mater. 2012;35:421–7. doi: 10.1016/j.conbuildmat.2012.04.013.
- [31] Saadoon T, Garcia A, Gómez-Meijide B. Dynamics of water evaporation in cold asphalt mixtures. Mater Des. 2017;134:196–206.
- [32] Lehmann P, Assouline S, Or D. Characteristic lengths affecting evaporative drying of porous media. Phys Rev E. 2008;77:1–16.
- [33] Abbas ZK, Abbood AA, Raghad S. Producing low-cost self-consolidation concrete using sustainable material. Open Eng. December 5, 2022;12(1):850–8.
- [34] Textofvideo. http://textofvideo.nptel.ac.in/105101084/lec7.pdf. Accessed date: 1 August 2018.
- [35] Norhidayah AH, Zul M, Mahmud H, Ramadhansyah PJ. Air void characterisation in porous asphalt using X-ray computed tomography. Paper presented at the Advanced Materials Research; 2014.

- [36] Muneam AK, Makki RF. Shear capacity of reinforced concrete beams with recycled steel fibers. Open Eng. 2023;13(1):20220457.
- [37] Xuping L. Recycling and reuse of waste concrete in China: Part I. Material behaviour of recycled aggregate concrete. Resour Conserv Recycling. 2008;53(1–2):36–44. doi: 10.1016/j.resconrec.2008.09.006.
- [38] Farid D, Said K. The use of coarse and fine crushed bricks as aggregate in concrete. Constr Build Mater. 2008;22:886–93. doi: 10.1016/j.conbuildmat.2006.12.013.
- [39] Faeze SK, Hadi A, Mostafa YR, Behzad K. An experimental study on the mechanical properties of underground mining backfill materials obtained from recycling of construction and demolition waste. Case Stud Constr Mater. 2023;18:e02046. doi: 10.1016/j. cscm.2023.e02046.
- [40] Qi G, Jianzhuang X, Jianyu S, Yiqing H, Jianmiao G. Properties of super-thin layer mortar with recycled brick fines for sintered perforated block masonry. Case Stud Constr Mater. 2023;18:e02015. doi: 10.1016/j.cscm.2023.e02015.
- [41] Yongcheng J, Dayang W. Constitutive model of waste brick concrete based on Weibull strength theory. Case Stud Constr Mater. 2023;18:e01738. doi: 10.1016/j.cscm.2022.e01738.
- [42] Garcia A, Hassn A, Chiarelli A, Dawson A. Multivariable analysis of potential evaporation from moist asphalt mixture. Constr Build Mater. 2015;98:80–8.